

Biological solution scattering: recent achievements and future challenges

J. Günter Grossmann

Received 16 August 2006

Accepted 2 February 2007

CCLRC Daresbury Laboratory, Molecular Biophysics Group, Warrington WA4 4AD, UK. Correspondence e-mail: j.g.grossmann@dl.ac.uk

In the post-genomic age it is apparent that as structures of larger macromolecules and their complexes are investigated, structure–function investigations are often confronted with the necessity to apply a portfolio of tools for biochemical and biophysical characterization. A survey of the published literature over the last decade reveals that publications in the area of structural biology employing neutron or X-ray scattering as one of their techniques tripled since 1995. Yet, taken as a whole, the contribution from small-angle scattering (SAS) to research papers dealing with structural analyses is still only of the order of 1% in 2005 (for comparison, less than 0.5% in 1995). Nevertheless, the last few years saw stimulating biological applications and analysis procedures which emphasize the growing potential of SAS applications for the structural studies of macromolecules in solution. The usage of SAS largely consists of low-resolution reconstructions of molecules with partial or without presumption of structural details, consistency analysis of high-resolution crystallographic structures and their corresponding low-resolution models determined in the solution state, and rigid-body refinement of multi-subunit assemblies including complexes and full-length multidomain proteins. Complementary structural information obtained from SAS in conjunction with data acquired by protein crystallography, NMR, molecular dynamics or computational docking provides a means to link low- and high-resolution models essential for the elucidation of biomolecular organization, interactions and function. The capabilities as well as limitations of determining low-resolution structures of multidomain proteins, macromolecular complexes and assemblies are highlighted in three examples. The first example is the characterization of the conformation of the PDZ region of SAP97, a multidomain protein involved in the regulation and localization of membrane receptor molecules. The second example is the characterization of the structural features of the TIM10 complex, an escort molecule for mitochondrial inner-membrane proteins, and the third example is the description of the shape and pH-induced conformational transition of a full-length bacterial potassium channel. The latter two in particular benefited from neutron scattering with contrast variation by using H–D labelling of the macromolecular complex or the solvent, respectively.

© 2007 International Union of Crystallography
Printed in Singapore – all rights reserved

1. Introduction

Solution X-ray and neutron scattering are complimentary techniques that can provide the size and shape of macromolecules with molecular masses ranging from a few kilodaltons to several million daltons. Even though scattering techniques do not have the high-resolution capability of protein crystallography (PX) or NMR, they are much more widely applicable to biological systems as long as monodisperse solutions are at hand. Thus, even intrinsically unstructured proteins can be evaluated by the scattering method, and very large complexes are also amenable. Despite being low-resolution methods, the ability to provide molecular dimensions and envelopes is especially important for establishing global information about partially folded, disordered or conformationally mobile states

of macromolecules under physiological conditions, such as those that occur in protein folding, multidomain molecules or multi-subunit complexes. In these cases, crystallization is challenging if not impossible and NMR studies give local rather than global structural information. The past decade has seen the appearance of data-analysis techniques which enable the reconstruction of molecular shapes from scattering data [see *e.g.* Svergun & Koch (2003) for a review]. Svergun & Stuhrmann (1991) were the first to show that it is feasible to obtain meaningful three-dimensional density maps from one-dimensional scattering data. Their remarkable procedure is capable of selecting an ensemble of consistent shapes from a large number of possible solutions. Several other approaches have since been tested successfully (Chacon *et al.*, 1998; Svergun, 1999; Walther *et al.*, 2000; Svergun *et al.*, 2001, Heller *et al.*, 2002); all of them treat

the scatterer as a system with a fixed number of connected scattering centres (an assembly of spheres) that form a more-or-less compact particle with a distinct solvent boundary. Disjointed centres or mixtures of different particles therefore do not meet the criteria for a biologically meaningful shape reconstruction. It is this approach of *ab initio* shape reconstruction in conjunction with scattering profile simulations and molecular modelling which has had a significant impact on the use of solution scattering techniques recently, as more valuable three-dimensional details can be extracted compared to results that merely hinge on quantities such as the radius of gyration, the maximum molecular dimension or on simple ellipsoidal or spherical conformational outlines. The currently available *ATSAS* software package developed and expanded by Svergun and co-workers (Konarev *et al.*, 2006) is popular with a large number of SAS users and is reaching a status similar to the software suite for PX (*CCP4*) a decade ago. Whether the threefold increase of published SAS papers in the area of structural biology (see Fig. 1) over the last decade is a result of these advances remains an open question. Regardless of the relatively low overall contribution (~1%) to structural studies, the significant contributions from a growing amount of SAS investigations can not be ignored.

The era of structural genomics results in an ever increasing archive of experimentally determined biological macromolecular three-dimensional structures at high resolution. Yet, despite the yearly growth of total structures in the Protein Data Bank (PDB), statistics show that 63% (85%) of structures deposited in the PDB (37 556 structures as of 4 July 2006) have molecular masses up to 50 kDa (100 kDa). Consequently, the representation of proteins consisting of one or a few domains seems to be adequate, whereas large macromolecules and complexes still indicate a challenge for structural genomics efforts. Inherent structural flexibility and the transient nature of complex formation represent significant barriers for high-resolution studies. Low-resolution information from SAS on macromolecules in solution can still provide valuable structure–function information not only in terms of *ab initio* shape determination but also in view of rigid-body modelling taking into account the knowl-

edge of a wealth of structures from small proteins and protein domains. In this context, it is worthwhile to briefly mention a few topical developments that are likely to provide stimuli for future directions of SAS applications. Petoukhov & Svergun (2005) describe methods to construct models of macromolecules and complexes from atomic information of subunits or domains against SAS data. The procedures allow, for instance, the addition of missing polypeptide segments (*e.g.* linkers between domains), exploitation of molecular symmetry and the consideration of information deduced from other techniques such as distance constraints between distinct residues. The latter is an essential validation criterion to select among multiple solutions that are otherwise in harmony with the experimental data. In a study of the Ras-specific nucleotide exchange factor SOS, Sondermann *et al.* (2005) employed X-ray scattering data to validate their computational docking models for this multidomain protein. The results were corroborated by other techniques. Similarly, Mattinen *et al.* (2002) showed that residual dipolar coupling information can reduce orientational degeneracy of shapes from multidomain proteins obtained by rigid-body modelling. This idea was taken forward significantly by Grishaev *et al.* (2005) who used SAS data as a constraint to complement high-resolution NMR structure determination. Considering the huge computational costs of fitting SAS data at each step of molecular dynamics and energy minimization during NMR structure refinement, a coarse-grain method was applied to decrease the structural complexity of amino acids (definition of ‘globs’ and associated correction factors to rectify the discrepancy between atomic and ‘glob’ scattering) and a reduced number of experimental data points to be fitted were taken into account. This led to a considerable reduction in the CPU time needed for the cross-validation of experimental and simulated scattering data. An analogous approach was reported recently by Wu *et al.* (2005), who used the X-ray scattering profile as a soft constraint to guide the folding of small helical proteins by computational methods.

In the following, three specific examples are presented in which the interplay between solution X-ray and neutron scattering and atomic structure information was exploited to extend low-resolution models towards pseudo high-resolution structures. Achievements are also discussed in the light of limitations and ensuing experimental and computational studies.

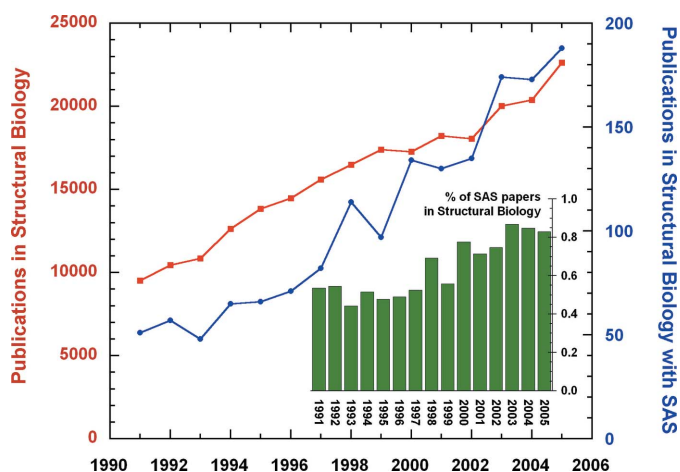


Figure 1 Upwards trend in the number of published SAS papers in the field of structural biology over the last 15 years. The results are displayed in absolute (main graph) and relative (inset) figures. The survey was performed with a search of the *ISI Web of Knowledge*SM publications database. For further comparison (not included in the above diagram), the number of papers with contributions from electron microscopy (EM) is almost four times the number of SAS publications in 2005, whereas a decade ago it was eight times the number of SAS publications. Moreover, the overall contributions of EM to structural biology papers decreased from 4% (in 1995) to 3% (in 2005).

2. Materials and methods

For sample preparation and explicit experimental details the reader is referred to the published literature given in the sections below. Specifically, Tim9, one of the two essential translocases for inner-membrane proteins (Tim9 and Tim10) that form part of the TIM10 complex, has been expressed in deuterated form at the ILL–EMBL–PSB Deuteration Laboratory in Grenoble, France. Subsequently, a functional complex was formed between deuterated Tim9 and hydrogenated Tim10, purified and dialysed against buffers of 40 and 100% D₂O/H₂O mixtures for neutron scattering studies. Neutron experiments were performed at instrument D22 (Institut Laue–Langevin, Grenoble, France). X-ray scattering experiments were carried out at beamline 2.1 of the UK Synchrotron Radiation Source at Daresbury. Concerning data reduction, this was carried out with software provided at the experimental facilities and for the subsequent analysis the *ATSAS* program package (Konarev *et al.*, 2006) was exploited. Molecular dynamics (MD) calculations on detergent and detergent–protein systems have been performed according to procedures as described *e.g.* in Bond & Sansom (2003) or Patargias *et*

al. (2005). Theoretical scattering patterns of the resulting MD structures have been compared with experimental profiles.

3. Results and discussion

3.1. Conformational features of the PDZ region of SAP97

SAP97 is a member of the membrane-associated guanylate kinase (MAGUK) family of proteins consisting of 911 residues, made up of three PDZ domains (~100 amino acids each) and a 'fused' SH3-GK domain. All these domains are common sites for protein-protein interactions, suggesting that SAP97 functions as a scaffold bringing together different proteins (*e.g.* ion channels) for information transfer. Structural knowledge so far relied on individual PDZ or SH3-GK domains; yet, the function of the protein involves all domains acting in concert. Even though long regions of flexibility are present in SAP97, the full-length protein was suggested to have a rather compact conformation in contrast to 'beads on a string'. X-ray scattering experiments were initiated to characterize the three SAP97 PDZ domains, in particular double and triple PDZ domain constructs (PDZ12: residues 218 to 406 and PDZ123: residues 218 to 577). The results reveal that PDZ12 is clearly smaller than PDZ123 ($R_g = 23.6 \pm 0.1 \text{ \AA}$, $D_{\max} = 75 \pm 3$ versus 33.3 ± 0.1 and $115 \pm 6 \text{ \AA}$, respectively). *Ab initio* shape calculations of the double domain show a dumbbell-shaped molecule with two distinct and apparently non-interacting domains; the triple domain is elongated, comprising three distinct components (Fig. 2). Nevertheless, considering the long linker between the second and third PDZ domain and an additional C-terminal segment, the scattering results still point to a rather compact shape for the triple domain. It was not expected to see the third PDZ domain in such close proximity to the other two domains. Rigid-body modelling allowed exploration of the spatial arrangement of domains together with plausible conformations for the mobile linker sections (Fig. 2). NMR data are consistent with the unstructured nature of the

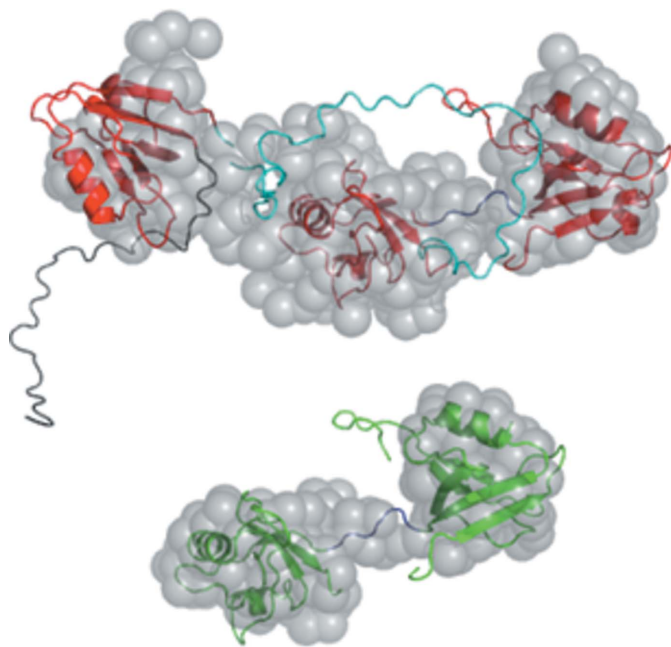


Figure 2

Ab initio shapes for double (PDZ12) and triple (PDZ123) domains restored from X-ray scattering data are displayed as transparent assemblies of spheres. Pseudo-atomic structures based on PDZ homology models and rigid-body modelling with addition of linkers [using the program *BUNCH* (Petoukhov & Svergun, 2005)] are superimposed in the form of ribbon drawings.

linker and C-terminal regions, and also confirm little short-range contacts among the globular PDZ domains (Goult *et al.*, 2007). It is remarkable that an extensive linker segment would keep the third PDZ domain in close proximity to the first and second PDZ domains. Therefore the unstructured linker is likely to induce transient interactions of PDZ3 with PDZ1 or PDZ2 which not only bring the PDZ domains closer together but may also assist in the organization and orientation of SAP97 domains and/or their interaction partners. Future experiments will concentrate on full-length SAP97 and its interaction complex with target proteins.

3.2. Structural characterization of the TIM10 chaperone complex

Protein import into the mitochondrion is mediated by specialized multi-protein machineries called translocases in both the outer and inner membrane. The TIM10 complex negotiates the aqueous divide between outer and inner membranes and thus specifically chaperones the inner-membrane insertion of hydrophobic proteins like the ADP/ATP carrier (AAC) that delivers ATP to the rest of the cell. The TIM10 complex is made of two proteins, Tim9 (89 residues) and Tim10 (90 residues). Despite their primarily helical secondary structure, their homodimeric association and four cysteine residues with the characteristic twin CX₃C motif, they only share a sequence identity of 21%. The functional TIM10 chaperone particle (60 kDa), which consists of three Tim9 and three Tim10 protomers, does not require ATP and as such is expected to adopt quite a distinct and novel structure. Solution X-ray scattering experiments provided the first glimpse of the size and shape of this complex (Fig. 3a and Lu *et al.*, 2004). With a largest dimension of around 90 Å, it can easily span at least half of the intermembrane space. The shape reconstruction was based on a threefold symmetry constraint based on the composition and properties of the constituent protomers Tim9 and Tim10 as well as the internal, three times repeated structurally related motif of the substrate (AAC). Accordingly, the low-resolution model shows characteristic features involving two types of protuberances that could be assigned to the six subunits forming the complex. Following biochemical deletion experiments together with X-ray scattering studies on these mutants, however, did not allow an assignment of the characteristic protuberances to either Tim9 or Tim10. In order to obtain more specific information on the organization of the subunits within the heterohexameric complex, neutron scattering data on TIM10 were collected with deuterated Tim9, which allowed the shape of Tim9 and Tim10 within the complex to be inferred. Examining the scattering at solvent contrasts of 40 and 100% D₂O/H₂O buffer solutions, the mixed deuterated-hydrogenated complex will show the predominant scattering contribution of Tim9 and Tim10, respectively (considering that the theoretical solvent contrast match points for hydrogenated and deuterated protein components are at ~42% and ~118% D₂O/H₂O mixtures; naturally, the solvent match point of 118% D₂O can experimentally not be achieved). Intriguingly, both scattering profiles show similar features and the overall structural parameters are comparable: $R_g = 30.1 \pm 0.5 \text{ \AA}$ and $D_{\max} = 88 \pm 5 \text{ \AA}$ in 40% D₂O, *i.e.* Tim10, and $R_g = 31.1 \pm 0.5 \text{ \AA}$ and $D_{\max} = 90 \pm 5 \text{ \AA}$ in 100% D₂O, *i.e.* Tim9 within the TIM10 complex. This result is also reflected in *ab initio* shape restorations based on threefold symmetry constraints (Fig. 3c,d). The characteristic protuberances that were identified in the original X-ray scattering experiments are still present but are comparable in size for both constituent components and the overall conformation adopts an oblate shape. According to this finding, Tim9 and Tim10 would behave structurally very similarly within the TIM10 complex. While the SAS data analysis was in progress, the high-resolution structure of the TIM10 complex was

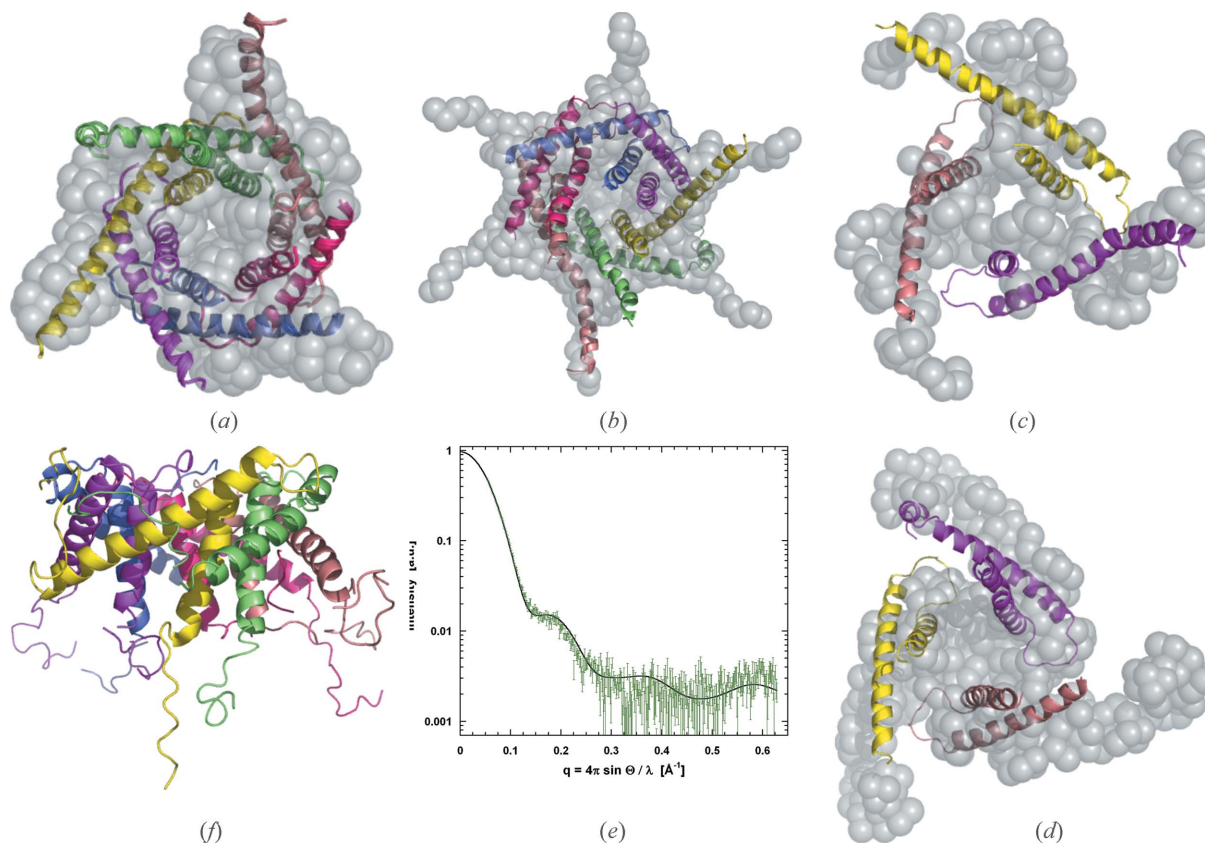


Figure 3 Shape reconstructions for the TIM10 complex based on three- (a) and sixfold (b) symmetry constraints compared with the superimposed ribbon model from the recently solved high-resolution structure. Shapes for Tim9 (c) and Tim10 (d) within the complex deduced from neutron contrast studies are also displayed, as well as the scattering profile simulation (e) calculated using the TIM10 crystal structure with added missing residues (f) restored by *BUNCH* and yielding a goodness-of-fit value of $\chi = 1.82$.

solved and published (Webb *et al.*, 2006) providing clarification of some of the structural peculiarities raised by the scattering results. So, the complex has a new architecture consisting of a six-bladed α -propeller, in which the alternate arrangement of Tim9 and Tim10 subunits produces a central ring with pseudo-sixfold symmetry. The propeller blades extend from this core like tentacles, breaking the symmetrical layout due to their inherent flexibility. The latter and the non-compactness of the overall structure in solution complicate a consistent *ab initio* shape reconstruction, as can be seen from a comparison with shapes based on three- and sixfold symmetry constraints (Fig. 3a,b). Yet there is an excellent agreement considering the evaluation of simulated and experimental scattering profiles (Fig. 3e). Further investigations concerning the interaction with and escorting of precursor proteins will capitalize on the TIM10 structure.

3.3. Shape analysis and simulations of the bacterial potassium channel KcsA

The bacterial potassium channel KcsA from *Streptomyces lividans* was used as a model system for structural and functional analysis of membrane protein channels, as it has proven extraordinarily accessible to structural studies (Sansom *et al.*, 2002). The successful isolation and purification of membrane proteins from their native state requires the substitution of the lipid bilayer by micelle-forming detergent molecules. Screening a series of detergents revealed that decyl- β -D-maltopyranoside (DM) not only solubilized KcsA well but also maintained the structural integrity of the channel tetramer in solution (Zimmer, 2003). Given the number of potassium channel

structures available, it provides a unique opportunity to understand the functional properties of a gated, ion-selective channel at the molecular level. Even though a mechanism of gating in the KcsA channel is beginning to emerge from a variety of techniques, the

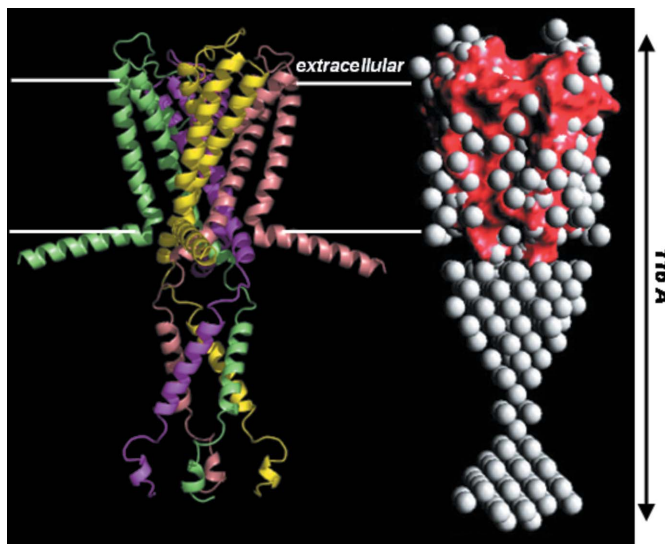


Figure 4 Proposed ribbon structure (left) and experimental shape (right) of full-length KcsA. The sphere model corresponds to the reconstructed shape from SANS data at maximum contrast (in 100% D₂O). The red space-filling model depicts the crystal structure of truncated KcsA that is imbedded in the membrane.

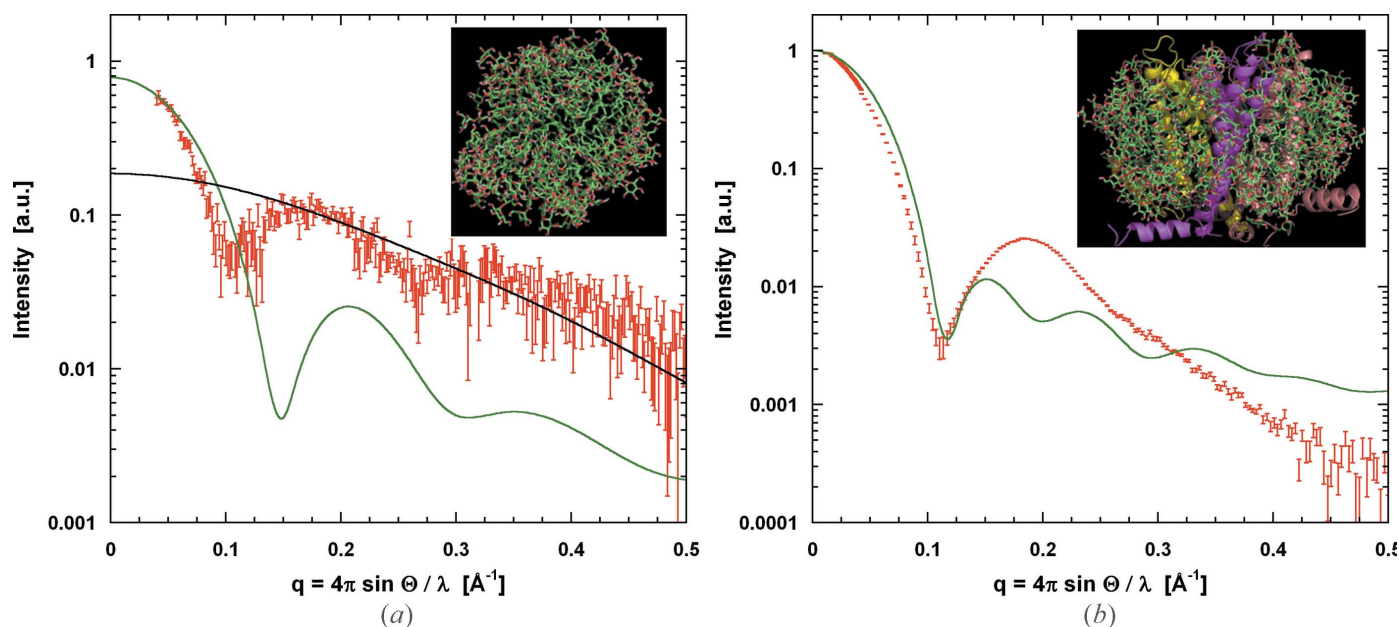


Figure 5 Scattering profile simulations based on MD snapshots of (a) a detergent micelle and (b) the truncated KcsA–detergent micelle complex. Corresponding X-ray scattering curves are given as red dots with error bars. The scattering from a single detergent (decyl- β -D-maltopyranoside) molecule is also displayed (black curve). The inset to (a) shows the micelle consisting of 94 detergent molecules and taken as snapshot after a 25 ns MD simulation with a diameter of about 60 Å. In contrast, the protein–detergent micelle comprises the truncated KcsA K⁺ channel (residues 1 to 124) enveloped in 138 detergent molecules. The structure was taken after a 10 ns simulation including the predicted helical KcsA N-terminal segment. The view shown in the inset to (b) is perpendicular to the channel's symmetry axis. Molecular graphics drawings were made with the program *PYMO*L (<http://pymol.sourceforge.net>).

structure of the full-length channel (including the C-terminal domain) has so far been elusive. The cytoplasmic C-terminal domain has been shown to play a critical role in the pH-dependent gating process (Cortes *et al.*, 2001). The bacterial K⁺ channel KcsA solubilized in DM was analysed by neutron and X-ray small-angle solution scattering (Zimmer *et al.*, 2006). Before the experiments, samples were dialysed for several hours in a 30 kDa cut-off membrane at room temperature against dialysis buffer containing 5 mM detergent [corresponding to about twice the critical micelle concentration (CMC) of DM, where the CMC refers to the total concentration of detergent that corresponds to the maximum possible concentration of detergent monomers in solution]. The C-terminally truncated version of KcsA, amenable for crystallographic studies, was compared with the full-length channel. Analysing the scattering data in terms of radius of gyration reveals differences between both KcsA species of up to 13.2 Å. Equally, the real-space distance distribution identifies a 40–50 Å extension of full-length KcsA compared to its C-terminally truncated counterpart. The X-ray and neutron scattering data are amenable for molecular shape reconstruction of full-length KcsA. The molecular envelopes calculated for full-length KcsA display an hourglass-shaped structure of the C-terminal domain (Fig. 4). The C-terminus extends the membrane spanning region of KcsA by 54 to 70 Å with a central constriction 10 to 30 Å wide. SAS was also used to characterize the KcsA channel under conditions favouring its open conformation. The solution scattering at pH 5.0 of full-length KcsA shows characteristics of a dumbbell-shaped macromolecular structure, originating from dimerization of the tetrameric K⁺ channel. Since C-terminally truncated KcsA measured under the same low pH conditions remains tetrameric, oligomerization of full-length KcsA seems to proceed *via* structurally changed C-terminal domains. The determined maximum dimensions of the newly formed complex increase by 50 to 60%. Shape reconstruction of the pseudo-octameric complex indicates the pH-induced conformational reorganization of the intracellular domain (Zimmer *et al.*, 2006). It is interesting to note

that the dimerization of the detergent-solubilized KcsA K⁺ channel at low pH most certainly is due to an *in vitro* effect. However, the observed dimerization is very likely stabilizing a conformation of the KcsA channel which *in vivo* might be achieved by the relevant interaction partner(s).

As a result of the close resemblance between restored shape and structural prediction for full-length KcsA (Fig. 4), which was underlined by simple scattering profile simulations (Zimmer *et al.*, 2006), more detailed simulations on KcsA were initiated based on MD calculations of membrane proteins and their interactions with detergents (Bond *et al.*, 2005; Bond & Sansom, 2006). As a first step, the simulation of a detergent micelle was attempted and compared to experimental findings. In view of the complexity and dynamic nature of the genuine detergent solution, the mediocre agreement between the simulated and experimental scattering curves is not unexpected (Fig. 5a). A significant amount of non-micelle-associated detergent molecules are likely to be present taking into account a DM solution with a concentration only slightly higher than the CMC. Moreover, the position of the first minimum in the experimental profile (Fig. 5a) would indicate that the shape of the detergent micelle is not as spherical as the MD simulation would suggest (see the inset to Fig. 5a). In fact, a study by Dupuy *et al.* (1997) indicates that β -maltoside molecules form oblate ellipsoidal micelles in water. Nevertheless, an attempt to simulate the detergent-solubilized truncated KcsA K⁺ channel was able to essentially reproduce the low-angle scattering features including the characteristic minimum near $q = 0.11 \text{ \AA}^{-1}$, where $q = (4\pi/\lambda) \sin \theta$, 2θ is the scattering angle and λ is the wavelength (Fig. 5b). Yet, the only fair agreement between experiment and simulation points also to a micelle conformation around the KcsA tetramer that is likely to be less spherical than the MD snapshot illustrates (inset to Fig. 5b). Consequently, comprehensive MD simulations will have to follow in order to analyse micellar size and shape characteristics as well as static and dynamic aspects of protein–detergent interactions. The SAS technique benefits from the nature

of these simulations, which will help to interpret the experimental data, but at the same time emerges as an appreciated experimental tool to provide feedback for the theoretical observations.

4. Conclusions

Considering the substantial advances in scattering-data-analysis methods for biological molecules in solution over the last decade, more complex and larger macromolecules can be meaningfully investigated with SAS. In view of the wealth of known high-resolution protein domain structures, the focus of scattering experiments will increasingly move from *ab initio* shape determination to rigid-body modelling of full-length multidomain proteins and multi-subunit complexes. Concomitantly, neutron contrast variation (in particular in the form of selectively labelled protein subunits), distance constraints between specific molecular surface areas (*e.g.* deduced from NMR or mutagenesis studies) and computer simulations will help to further reduce ambiguities so as to arrive at biologically relevant and unique results. Along with findings from other techniques, the collective information will permit crucial insights into challenging questions of structural biology to be gained, such as the origins of aberrant protein structure–function relationships and their consequences in human diseases. Moreover, with the continuing enhancements in high-performance computing, SAS data ought to become a convenient assessment and a viable constraint for molecular dynamics simulations. These advancements are expected to raise the profile of SAS, pushing the percentage of publications in structural biology with contributions from SAS towards the 5% margin.

The solution scattering investigations would not have been possible without the enthusiasm, interest and encouragement of several collaborators and colleagues: Professor Lu-Yun Lian and her group at Liverpool University (PDZ domains), Dr Kostas Tokatlidis and his group at the University of Crete (TIM10 chaperone complex) and Drs Declan Doyle and Jochen Zimmer at Oxford University (bacterial potassium channel, KcsA). The KcsA study initiated MD simulations of protein–micelle interactions in Professor Mark Sansom's group (with Drs Peter Bond and Zara Sands) at Oxford University. My appreciation also goes to Dr Peter Timmins at the ILL for his support, not only during neutron scattering experiments, and Dr Michael Haertlein and the staff at the ILL–EMBL–PSB

Deuteration Laboratory in Grenoble, which enabled the labelling of the TIM10 complex. Last but not least I would like to thank my colleagues at the Daresbury SRS as well as the support and funding from CCLRC Daresbury Laboratory.

References

- Bond, P. J., Cuthbertson, J. & Sansom, M. S. P. (2005). *Biochem. Soc. Trans.* **33**, 910–912.
- Bond, P. J. & Sansom, M. S. P. (2003). *J. Mol. Biol.* **329**, 1035–1053.
- Bond, P. J. & Sansom, M. S. P. (2006). *J. Am. Chem. Soc.* **128**, 2697–2704.
- Chacon, P., Moran, F., Diaz, J. F., Pantos, E. & Andreu, J. M. (1998). *Biophys. J.* **74**, 2760–2775.
- Cortes, D. M., Cuello, L. G. & Perozo, E. (2001). *J. Gen. Physiol.* **117**, 165–180.
- Dupuy, C., Auvray, X., Petipas, C., Rico-Lattes, I. & Lattes, A. (1997). *Langmuir*, **13**, 3965–3967.
- Goult, B. T., Rapley, J. D., Golovanova, M., Sampson, L. J., Dart, C., Kitmitto, A., Grossmann, J. G., Leyland, M. L. & Lian, L.-Y. (2007). *Biochemistry*. Submitted.
- Grishaev, A., Wu, J., Trehwella, J. & Bax, A. (2005). *J. Am. Chem. Soc.* **127**, 16621–16628.
- Heller, W. T., Abusamhadneh, E., Finley, N., Rosevear, P. R. & Trehwella, J. (2002). *Biochemistry*, **41**, 15654–15663.
- Konarev, P. V., Petoukhov, M. V., Volkov, V. V. & Svergun, D. I. (2006). *J. Appl. Cryst.* **39**, 277–286.
- Lu, H., Golovanov, A. P., Alcock, F., Grossmann, J. G., Allen, S., Lian, L.-Y. & Tokatlidis, K. (2004). *J. Biol. Chem.* **279**, 18959–18966.
- Mattinen, M.-L., Pääkkönen, K., Ikonen, T., Craven, J., Drakenberg, T., Serimaa, R., Waltho, J. & Annala, A. (2002). *Biophys. J.* **83**, 1177–1183.
- Patargias, G., Bond, P. J., Deol, S. S. & Sansom, M. S. P. (2005). *J. Phys. Chem.* **B109**, 575–582.
- Petoukhov, M. V. & Svergun, D. I. (2005). *Biophys. J.* **89**, 1237–1250.
- Sansom, M. S. P., Shrivastava, I. H., Bright, J. N., Tate, J., Capener, C. E. & Biggin, P. C. (2002). *Biochim. Biophys. Acta*, **1565**, 294–307.
- Sondermann, H., Nagar, B., Bar-Sagi, D. & Kuriyan, J. (2005). *Proc. Natl Acad. Sci. USA*, **102**, 16632–16637.
- Svergun, D. I. (1999). *Biophys. J.* **76**, 2879–2886.
- Svergun, D. I. & Koch, M. H. J. (2003). *Rep. Prog. Phys.* **66**, 1735–1782.
- Svergun, D. I., Petoukhov, M. V. & Koch, M. H. J. (2001). *Biophys. J.* **80**, 2946–2953.
- Svergun, D. I. & Stuhmann, H. B. (1991). *Acta Cryst.* **A47**, 736–744.
- Waltho, D., Cohen, F. E. & Doniach, S. (2000). *J. Appl. Cryst.* **33**, 350–363.
- Webb, C. T., Gorman, M. A., Lazarou, M., Ryan, M. T. & Gulbis, J. M. (2006). *Mol. Cell*, **21**, 123–133.
- Wu, Y., Tian, X., Lu, M., Chen, M., Wang, Q. & Ma, J. (2005). *Structure*, **13**, 1587–1597.
- Zimmer, J. (2003). PhD Thesis, Department of Biochemistry, University of Oxford.
- Zimmer, J., Doyle, D. A. & Grossmann, J. G. (2006). *Biophys. J.* **90**, 1752–1766.